Soluble Synthetic Multiporphyrin Arrays. 2. Photodynamics of Energy-Transfer Processes

Jiunn-Shyong Hsiao,[#] Brent P. Krueger,[¶] Richard W. Wagner,[†] Thomas E. Johnson,[†] John K. Delaney,[‡] David C. Mauzerall,[‡] Graham R. Fleming,[¶] Jonathan S. Lindsey,*[,†] David F. Bocian,*[,§] and Robert J. Donohoe*[,#]

Contribution from the Biochemistry and Biotechnology Group, CST-4, MS C345, Los Alamos National Laboratory, Los Alamos, New Mexico 87545, Department of Chemistry and The James Franck Institute, University of Chicago, 5735 S. Ellis Avenue, Chicago, Illinois 60637, Department of Chemistry, North Carolina State University, Raleigh, North Carolina 27695, The Rockefeller University, 1230 York Avenue, New York, New York 10021, and Department of Chemistry, University of California, Riverside, California 92521

Received May 14, 1996[⊗]

Abstract: Soluble ethyne-linked tetraarylporphyrin arrays that mimic natural light-harvesting complexes by absorbing light and directing excited-state energy have been investigated by static and time-resolved absorption and fluorescence spectroscopies. Of particular interest is the role of the diarylethyne linkers in mediating energy transfer. The major conclusions from this study, which is limited to the examination of arrays containing Zn and free-base (Fb) porphyrins, include the following: (1) Singlet excited-state energy transfer from the Zn porphyrin to the Fb porphyrin is extremely efficient (95−99%). Competitive electron-transfer reactions are not observed. (2) The rate of energy transfer is slowed up to 4-fold by the addition of groups to the linker that limit the ability of the linker and porphyrin to adopt geometries tending toward coplanarity. Thus, the mechanism of energy transfer predominantly involves through-bond communication via the linker. Consistent with this notion, the measured lifetimes of the Zn porphyrin in the dimers at room temperature yield energy-transfer rates ($(88\ \text{ps})^{-1} < k_{\text{trans}} < (24\ \text{ps})^{-1}$) that are significantly faster than those predicted by the Förster (through-space) mechanism ($(720\ \text{ps})^{-1}$). Nevertheless, the electronic communication is weak and the individual porphyrins appear to retain their intrinsic radiative and non-radiative rates upon incorporation into the arrays. (3) Transient absorption data indicate that the energy-transfer rate between two isoenergetic Zn porphyrins in a linear trimeric array terminated by a Fb porphyrin is $(52 \pm 19\ \text{ps})^{-1}$ in toluene at room temperature, while the time-resolved fluorescence data suggest that it may be significantly faster. Accordingly, incorporation of multiple isoenergetic pigments in extended linear or two-dimensional arrays will permit efficient overall energy transfer. (4) Medium effects, including variations in solvent polarity, temperature, viscosity, and axial solvent ligation, only very weakly alter (≤2.5-fold) the energy-transfer rates. However, the Fb porphyrin fluorescence in the Zn−Fb dimers is quenched in the polar solvent dimethyl sulfoxide (but not in toluene, castor oil, or acetone), which is attributed to charge-transfer with the neighboring Zn porphyrin following energy transfer. Collectively, the studies demonstrate that extended multiporphyrin arrays can be designed in a rational manner with predictable photophysical features and efficient light-harvesting properties through use of the diarylethyne-linked porphyrin motif.

I. Introduction

Photosynthesis begins with absorption of dilute sunlight by pigments in light-harvesting antenna complexes. Upon excitation, energy migration occurs among these pigments until a reaction center is encountered, where charge separation occurs. The energy migration process is extraordinarily rapid and can involve hundreds of pigments.[1] Artificial reaction centers designed to investigate photoinduced charge separation have been the target of numerous synthetic, spectroscopic, and theoretical studies.[2] The design and characterization of synthetic analogs of the light-harvesting complexes have received less attention. Such mimics of the antennae hold promise for applications in solar energy collection and utilization and may serve in molecular-scale information-processing applications.[3]

A prevalent strategy in the design of synthetic light-harvesting model systems is the incorporation of covalently linked porphyrins (metallo and free base) as mimics of the natural photosynthetic pigments. A variety of such arrays, spanning the range of 3-dimensional architecture, structural rigidity, nature of the linker, and degree of inter-chromophore electronic

[#] Los Alamos National Laboratory.
[¶] University of Chicago.
[†] North Carolina State University.
[‡] Rockefeller University.
[§] University of California.
[⊗] Abstract published in *Advance ACS Abstracts*, November 1, 1996.

(1) (a) Larkum, A. W. D.; Barrett, J. *Adv. Bot. Res.* **1983**, *10*, 1−219. (b) *Photosynthetic Light-Harvesting Systems*; Scheer, H., Siegried, S., Eds.; W. de Gruyter: Berlin 1988. (c) Mauzerall, D. C.; Greenbaum, N. L. *Biochim. Biophys. Acta* **1989**, *974*, 119−140. (d) Hunter, C. N.; van Grondelle, R.; Olsen, J. D. *Trends Biochem. Sci.* **1989**, *14*, 72−76. (e) McDermott, G.; Prince, S. M.; Freer, A. A.; Hawethornthwaite-Lawless, A. M.; Papiz, M. Z.; Cogdell, R. J.; Isaacs, N. W. *Nature* **1995**, *374*, 517−521. (f) Karrasch, S.; Bullough, P. A.; Ghosh, R. *EMBO J.* **1995**, *14*, 631−638.

(2) For reviews, see: (a) Boxer, S. G. *Biochim. Biophys. Acta* **1983**, *726*, 265−292. (b) Gust, D.; Moore, T. A. *Science* **1989**, *244*, 35−41. (c) Borovkov, V. V.; Evstigneeva, R. P.; Strekova, L. N.; Filippovich, E. I. *Russ. Chem. Rev.* **1989**, *58*, 602−619. (d) Gust, D.; Moore, T. A. *Top. Curr. Chem.* **1991**, *159*, 103−151. (e) Wasielewski, M. R. In *Chlorophylls*; Scheer, H., Ed.; CRC Press: Boca Raton, FL, **1991**; pp 269−286. (f) Wasielewski, M. R. *Chem. Rev.* **1992**, *92*, 435−461. (g) Gust, D.; Moore, T. A.; Moore, A. L. *Acc. Chem. Res.* **1993**, *26*, 198−205. (h) Gribkova, S. E.; Evstigneeva, R. P.; Luzgina, V. N. *Russ. Chem. Rev.* **1993**, *62*, 963−979. (i) Kurreck, H.; Huber, M. *Angew. Chem., Int. Ed. Engl.* **1995**, *34*, 849−866.

(3) (a) Liu, C-Y.; Pan, H-L; Fox, M. A.; Bard, A. J. *Science* **1993**, *261*, 897−899. (b) Kay, A.; Grätzel, M. *J. Phys. Chem.* **1993**, *97*, 6272−6277.

S0002-7863(96)01612-5 CCC: $12.00

coupling, have been reported to undergo intramolecular porphyrin−porphyrin energy transfer.[4−29] Other porphyrin arrays joined directly by ethyne or butadiyne linkers have dramatically altered absorption spectra, indicating very strong electronic coupling.[30−39] The majority of these arrays are bichromophoric and have been synthesized via routes that are not amenable to the preparation of extended multiporphyrin arrays. It is desirable to select a molecular design that can predictably yield efficient excited-state energy transfer and that is compatible with the synthesis of multiporphyrin arrays. Further, the molecular design should maintain some of the individual aspects of the individual chromophores within the arrays (so that the resulting complex has predictable characteristics) while imparting efficient electronic communication channels among the chromophores. One of our groups has developed a building block approach that meets these fundamental needs and also offers versatile solubilities and molecular architectures.[22,40] The arrays are constructed with an ethyne linkage between aryl groups on adjacent tetraarylporphyrin macrocycles, which provides a semirigid architecture that limits direct chromophore interactions. The center-to-center and edge-to-edge distances for the porphyrins in these systems are approximately 20 and 13.5 Å, respectively. The array geometry does have some solution flexibility, including free rotation about the ethyne and limited bending of the linker.[41] The ground state absorption spectra of all the diarylethyne linked arrays are nearly a composite of the absorption spectra of the individual pigments (limited here to Zn and free base (Fb) porphyrins), suggesting that the electronic coupling of the porphyrin chromophores is weak. Weak coupling preserves the character of the individual pigments but also increases the possibility of inefficient energy transfer. Nevertheless, emission data from selected arrays indicate that the excited state energy-transfer yields from the Zn to Fb porphyrin are over 90%.[22,23] Resonance Raman studies of the neutral arrays and EPR investigations of the oxidized arrays indicate through-bond electronic communication via the linkers.[42] The weak coupling has allowed construction of light-harvesting arrays,[22] a molecular photonic wire,[23] and molecular optoelectronic gates,[29] all of which exhibit efficient excited-state energy transfer.

The goals of the present work are to determine the rates, efficiencies, and mechanisms of energy transfer and investigate how these are affected by structural alteration of the linker as well as changes in the medium. A starting point for understanding the energy-transfer processes in extended, multiporphyrin arrays is examination of the respective pairwise interactions among porphyrins. We have designed and prepared a family of dimeric and trimeric molecules for investigating these issues, as described in the previous companion paper.[41] In this report, the photodynamics of dimeric and trimeric arrays containing Zn and Fb porphyrins are investigated by static and time-resolved absorption and fluorescence spectroscopies. The porphyrin monomers that comprise the arrays are shown in Chart 1. The dimers incorporate a Zn porphyrin and a Fb porphyrin connected by the diarylethyne linker, as shown in Chart 2. The shorthand nomenclature used in the text is provided in the charts. The dimer with the unhindered linker is denoted ZnFbU. The dimer with torsionally constraining methyl groups attached on the linker aryl group adjacent to the Zn porphyrin is designated the proximally-hindered dimer, ZnFbP, as the Zn porphyrin transfers energy to the Fb porphyrin. The other two dimers are the distally-hindered dimer, ZnFbD, and the bis-hindered dimer, ZnFbB. Chart 3 shows a dimer and a trimer composed of all-Zn porphyrins, and a trimer with two consecutive Zn porphyrins terminated by a Fb porphyrin, ZnZnFb, in which the linker is unhindered between the two Zn porphyrins and proximally hindered between the Zn and Fb porphyrins. A subsequent companion paper explores electronic communication

(4) Schwarz, F. P.; Gouterman, M.; Muljiani, Z.; Dolphin, D. H. *Bioinorg. Chem*. **1972**, *2*, 1−32.
(5) Anton, J. A.; Loach, P. A.; Govindjee *Photochem. Photobiol*. **1978**, *28*, 235−242.
(6) Selensky, R.; Holten, D.; Windsor, M. W.; Paine, J. B., III; Dolphin, D.; Gouterman, M.; Thomas, J. C. *Chem. Phys.* **1981**, *60*, 33−46.
(7) Wasielewski, M. R.; Niemczyk, M. P.; Svec, W. A. *Tetrahedron Lett.* **1982**, *23*, 3215−3218.
(8) Mialocq, J. C.; Giannotti, C.; Maillard, P.; Momenteau, M. *Chem. Phys. Lett.* **1984**, *112*, 87−93.
(9) Regev, A.; Galili, T.; Levanon, H.; Harriman, A. *Chem. Phys. Lett.* **1986**, *131*, 140−146.
(10) Gonen, O.; Levanon, H. *J. Chem. Phys.* **1986**, *84*, 4132−4141.
(11) Brookfield, R. L.; Ellul, H.; Harriman, A.; Porter, G. *J. Chem. Soc., Faraday Trans. 2* **1986**, *82*, 219−233.
(12) Davila, J.; Harriman, A.; Milgrom, L. R. *Chem. Phys. Lett.* **1987**, *136*, 427−430.
(13) Chardon-Noblat, S.; Sauvage, J.-P.; Mathis, P. *Angew. Chem., Int. Ed. Engl.* **1989**, *28*, 593−595.
(14) Rempel, U.; Von Maltzan, B.; Von Borczyskowski, C. *Chem. Phys. Lett.* **1990**, *169*, 347−354.
(15) Osuka, A.; Maruyama, K.; Yamazaki, I.; Tamai, N. *Chem. Phys. Lett.* **1990**, *165*, 392−396.
(16) Osuka, A.; Nagata, T.; Maruyama, K.; Mataga, N.; Asahi, T.; Yamazaki, I.; Nishimura, Y. *Chem. Phys. Lett.* **1991**, *185*, 88−94.
(17) Gust, D.; Moore, T. A.; Moore, A. L.; Gao, F.; Luttrull, D.; DeGraziano, J. M.; Ma, X. C.; Makings, L. R.; Lee, S-J.; Trier, T. T.; Bittersmann, E.; Seely, G. R.; Woodward, S.; Bensasson, R. V.; Rougée, M.; De Schryver, F. C.; Van der Auweraer, M. *J. Am. Chem. Soc.* **1991**, *113*, 3638−3649.
(18) Gust, D.; Moore, T. A.; Moore, A. L.; Leggett, L.; Lin, S.; DeGraziano, J. M.; Hermant, R. M.; Nicodem, D.; Craig, P.; Seely, G. R.; Nieman, R. A. *J. Phys. Chem.* **1993**, *97*, 7926−7931.
(19) Tamiaki, H.; Nomura, K.; Maruyama, K. *Bull. Chem. Soc. Jpn.* **1993**, *66*, 3062−3068.
(20) Osuka, A.; Nakajima, S.; Maruyama, K.; Mataga, N.; Asahi, T.; Yamazaki, I.; Nishimura, Y.; Ohno, T.; Nozaki, K. *J. Am. Chem. Soc.* **1993**, *115*, 4577−4589.
(21) Sessler, J. L.; Capuano, V. L.; Harriman, A. *J. Am. Chem. Soc.* **1993**, *115*, 4618−4628.
(22) Prathapan, S.; Johnson, T. E.; Lindsey, J. S. *J. Am. Chem. Soc*. **1993**, *115*, 7519−7520.
(23) Wagner, R. W.; Lindsey, J. S. *J. Am. Chem. Soc*. **1994**, *116*, 9759−9760.
(24) DeGraziano, J. M.; Liddell, P. A.; Leggett, L.; Moore, A. L.; Moore, T. A.; Gust, D. *J. Phys. Chem.* **1994**, *98*, 1758−1761.
(25) Tamiaki, H.; Nomura, K.; Maruyama, K. *Bull. Chem. Soc. Jpn.* **1994**, *67*, 1863−1871.
(26) Harriman, A.; Heitz, V.; Ebersole, M.; van Willigen, H. *J. Phys. Chem.* **1994**, *98*, 4982−4989.
(27) Iida, K.; Nango, M.; Okada, K.; Hikita, M.; Matsuura, M.; Kurihara, T.; Tajima, T.; Hattori, A.; Ishikawa, S.; Yamashita, K.; Tsuda, K.; Kurono, Y. *Bull. Chem. Soc. Jpn.* **1995**, *68*, 1959−1968.
(28) Osuka, A.; Tanabe, N.; Kawabata, S.; Yamazaki, I.; Nishimura, Y. *J. Org. Chem.* **1995**, *60*, 7177−7185.
(29) Wagner, R. W.; Lindsey, J. S.; Seth, J.; Palaniappan, V.; Bocian, D. F. *J. Am. Chem. Soc*. **1996**, *118*, 3996−3997.
(30) Arnold, D. P.; Johnson, A. W.; Mahendran, M. *J. Chem. Soc., Perkin Trans. 1* **1978**, 366−370.
(31) Arnold, D. P.; Nitschinsk, L. J. *Tetrahedron* **1992**, *48*, 8781−8792.
(32) Arnold, D. P.; Nitschinsk, L. J. *Tetrahedron Lett.* **1993**, *34*, 693−696.
(33) Arnold, D. P.; James, D. A.; Kennard, C. H. L.; Smith, G. *J. Chem. Soc., Chem. Commun.* **1994**, 2131−2132.
(34) Anderson, S.; Martin, S. J.; Bradley, D. D. C. *Angew. Chem., Int. Ed. Engl.* **1994**, *33*, 655−657.
(35) Anderson, H. L. *Inorg. Chem.* **1994**, *33*, 972−981.
(36) Gosper, J. J.; Ali, M. *J. Chem. Soc., Chem. Commun.* **1994**, 1707−1708.
(37) Lin, V. S.-Y.; DiMagno, S. G.; Therien, M. J. *Science* **1994**, *264*, 1105−1111.
(38) Angiolillo, P. J.; Lin, V. S.-Y.; Vanderkooi, J. M.; Therien, M. J. *J. Am. Chem. Soc.* **1995**, *117*, 12514−12527.
(39) Lin, V. S.-Y.; Therien, M. J. *Chem. Eur. J.* **1995**, *1*, 645−651.
(40) Paper 1 of this series: Wagner, R. W.; Johnson, T. E.; Lindsey, J. S. *J. Am. Chem. Soc*. **1996**, *118*, 11166−11180.
(41) Bothner-By, A.; Dadok, J.; Johnson, T. E.; Lindsey, J. S. *J. Phys. Chem.* In press.
(42) Seth, J.; Palaniappan, V.; Johnson, T. E.; Prathapan, S.; Lindsey, J. S.; Bocian, D. F. *J. Am. Chem. Soc*. **1994**, *116*, 10578−10592.

Chart 1. Porphyrin Monomers

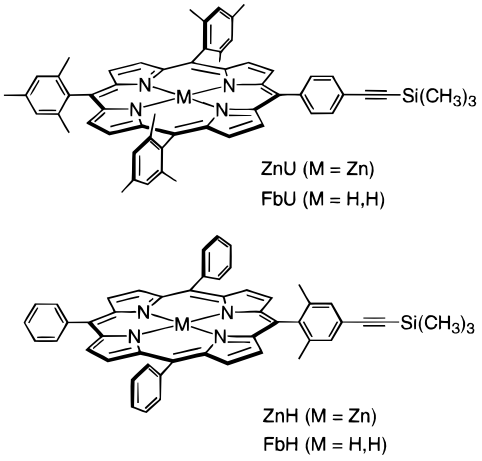

Chart 2. ZnFb Dimers with Different Linkers

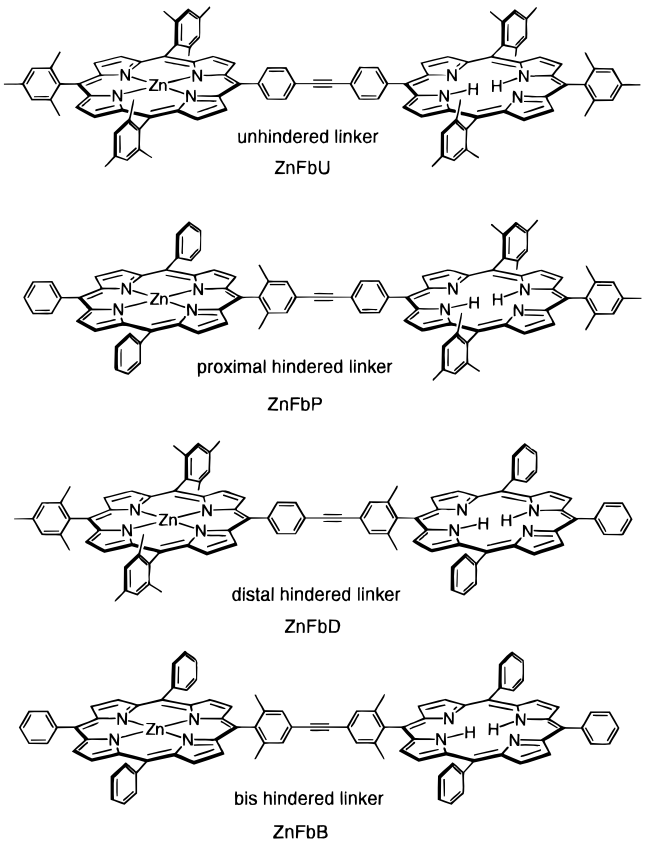

pathways, focusing on the ground-state resonance Raman and absorption spectroscopy of neutral arrays and the EPR spectroscopy of oxidized arrays.[43]

II. Experimental Section

A. Sample Preparation and Integrity. The purity of the isolated arrays is ≥99%.[40] During early work the purity of the arrays was ~95%, but we identified residual Zn and Fb porphyrin monomers that could be removed with improved purification methods, yielding the arrays with ≥99% purity whose photochemical properties are reported here. A small amount (≤1%) of residual Zn porphyrin monomer could not be removed, however, and this component appears as a residual (~2-ns lifetime) in the fluorescence decays of all of the ZnFb dimers and the ZnZnFb trimer. Spectroscopic grade solvents were used for all of the optical studies reported herein. The solvents and their static dielectric constants at room temperature (parentheses) are as follows: toluene (2.38), *n*-butylbenzene (2.36), castor oil (the static dielectric constant is not known, but is likely to lie between that of *n*-butylbenzene and ethyl acetate), ethyl acetate (6.02), acetone (20.7), and dimethyl sulfoxide (DMSO) (46.7).[44] Castor oil, a triglyceride of long-chain oleic acids, is distinguished from the other solvents by its high viscosity at room temperature (650 cP compared with 0.55 cP for toluene).[45] The multiporphyrin arrays are highly soluble in castor oil. Samples in castor oil were prepared by using a 10−20 μL toluene stock solution of the porphyrin or array which was added to 2.5−3 mL of castor oil in a cuvette. The cuvette was then warmed in a hot-water bath at 80 °C and occasionally shaken until a homogeneous solution was obtained. With the exception of those in castor oil, all samples were degassed by bubbling with N_2 prior to use. In order to confirm the integrity of the samples, absorption spectra were examined both before and after the pulsed laser experiments. These measurements did not reveal the presence of aggregation or decomposition of the samples, which suggests that the arrays are photostable.

B. Static Absorption and Fluorescence Spectroscopy. Absorption, emission, and excitation spectra, including measurements of extinction coefficients and emission quantum yields, were determined at room temperature. Absorption spectra were collected using a Varian Cary 3 with 1 nm band widths and 0.25 nm data intervals. The extinction coefficients for the porphyrin monomers in toluene at room temperature have been determined at the Soret band and at the wavelengths for photochemical excitation (listed at the Soret, 532, 550, and 587 nm): FbU 431000, 4580, 7800, 3880; FbH 472600, 5170, 8900, 5710; ZnU, 468000, 5890, 23725, 2900; ZnH 499200, 6460, 24350, 3480 (all in M^{-1} cm^{-1}). Fluorescence spectra were collected using a Spex Fluoromax with 1 mm slit widths (4.25 nm) and 1 nm data intervals. Emission spectra were corrected for instrument response and obtained with $A_{\lambda_{exc}} < 0.1$. Quantum yields were determined by ratioing integrated corrected emission spectra to ZnTPP (0.030) or TPP (0.11) in toluene.[46] Fluorescence quantum yield measurements in other solvents were corrected for refractive index differences relative to toluene.[47]

C. Time-Resolved Fluorescence Spectroscopy. Fluorescence lifetimes were measured at the Rockefeller University using an instrument which allows rapid determination of lifetimes and time shifts in emission. This instrument was used in a 1-week period to survey the entire set of these and many related compounds in various solvents and at different temperatures. The samples were excited by 30-ps (fwhm) pulses at 532 nm from a mode-locked Nd-YAG laser (Continuum) and the emission was detected using a microchannel plate photomultiplier (Hamamatsu R1294-01). The resulting transient signal was digitized (10 ps per point) by a scan converter (Tektronix 7912AD) and a computer. In each experiment 64-128 data scans were collected at 10 Hz. The microchannel plate response time is ~1 ns but the system stability allows deconvolution of lifetimes less than 100 ps with an uncertainty of ±30 ps. Fluorescence lifetimes were collected at 600 or 610 nm on the 5 or 10 ns time scale and at 725 nm on the 5 or 50 ns time scale using interference notch band filters. Fluorescence decays were fitted by iterative deconvolution using the instrument response function measured at 530 nm.[48] Samples were prepared to an optical density of approximately 0.05 to 0.1 at 532 nm.

Fluorescence lifetimes reported in this paper (with the exception of those for a few porphyrin monomers) were measured at the University of Chicago with a time-correlated single-photon counting system described previously.[49] Excitation light was provided by a Rhodamine 560 (Exciton) dye laser (Coherent 590) synchronously pumped by the 514 nm line of a mode-locked argon ion laser (Coherent Innova 200) operating at 76 MHz. The dye laser was tuned to 560 ± 2 nm and

(43) Paper 3 of this series: Seth, J.; Palaniappan, V.; Wagner, R. W.; Johnson, T. E.; Lindsey, J. S.; Bocian, D. F. *J. Am. Chem. Soc.* **1996**, *118*, 11194−11207.

(44) Riddick, J. A.; Bunger, W. B. *Organic Solvents*, 3rd ed.; Techniques of Chemistry, Vol. II; Wiley-Interscience: New York, 1970.

(45) *CRC Handbook Of Tables For Applied Engineering Science*, 2nd ed.; Bolz, R. E., Tuve, G. L., Eds.; CRC Press: Cleveland, 1973; p 92.

(46) Seybold, P. G.; Gouterman, M. *J. Mol. Spectrosc.* **1969**, *31*, 1−13.

(47) Ediger, M. D.; Moog, R. S.; Boxer, S. G.; Fayer, M. D. *Chem. Phys. Lett.* **1982**, *88*, 123−127.

(48) Mauzerall, D. C. *Biochim. Biophys. Acta* **1985**, *809*, 11−16.

(49) Chang, M. C.; Courtney, S. H.; Cross, A. J.; Gulotty, R. J.; Petrich, J. W.; Fleming, G. R. *Anal. Instrum.* **1985**, *14*, 433−464.

Chart 3. Arrays for Study of Energy Transfer among Isoenergetic Porphyrins

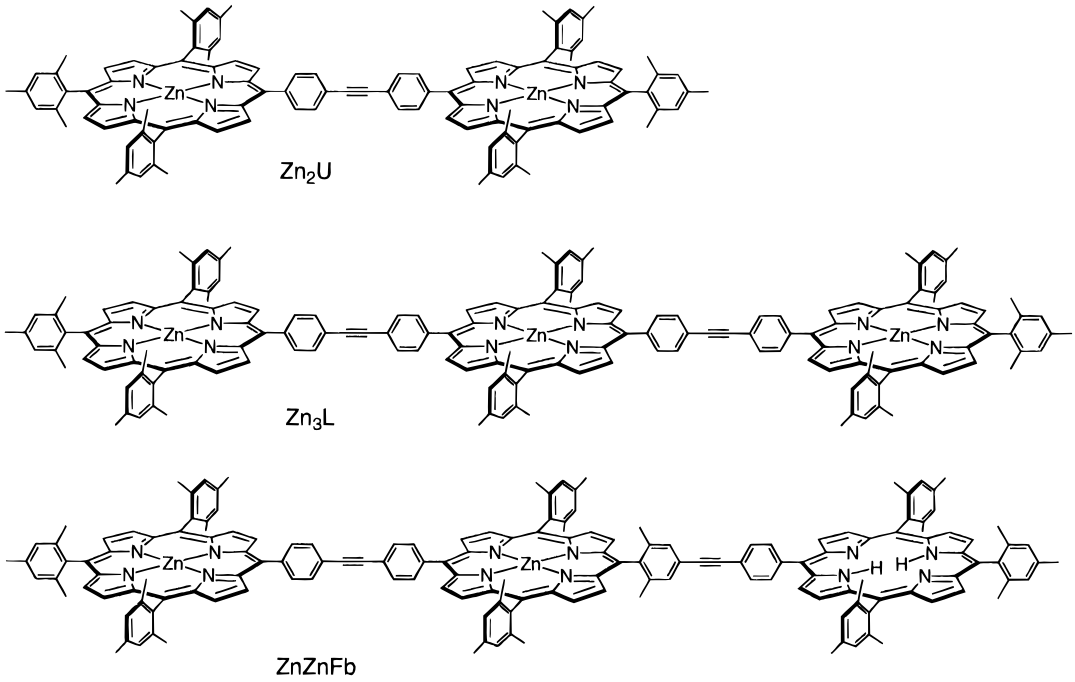

cavity dumped at 3.8 MHz. Samples were prepared in toluene and other solvents to an optical density of approximately 0.1 at 560 nm in a 1 cm path length cell. Samples other than those prepared in castor oil, which was too viscous, were stirred throughout data collection by a magnetic stir bar. After passing through a 0.75 mm slit adjacent to the sample, the emission signal was detected orthogonal to the excitation beam. Subsequently, the emission passed through a polarizer oriented at the magic angle relative to the vertically polarized excitation. A long pass filter (Schott OG580) was used to remove scattered excitation before the emission was focused into a monochromator (band pass 8 nm) set to the desired detection wavelength which varied slightly depending on sample and solvent. Monomer emission was observed at the emission peak near 650 nm. In the dimers, the rapid Zn decay component was observed at the Zn emission peak near 600 nm while the long Fb decay component was observed at the Fb emission peak near 650 nm. The emission was detected by a fast multichannel plate/photomultiplier tube. Pulse energy at the sample was varied from 0.5 to 3 nJ (~1 mm diameter collimated beam) without substantial change in the decay curves. Acquisition times were 20−40 s for instrument response functions and 3−30 min for emission decay curves. Instrument response functions were taken before and after every emission decay measurement by replacing the sample with a scattering solution of nondairy creamer in water (0.1 optical density) and tuning the monochromator to the laser wavelength. A typical instrument response function exhibited a fwhm of 85 ps and a full width at 1/10 maximum of 270 ps. Model decay curves were fitted to the emission decays by convolution with the instrument response functions and iterative comparison by a nonlinear least squares algorithm. The monomer data were fit using single exponential decays, while the dimer data were fit using triple exponential decays. After the best fit had been found, error bars for the decay times were determined by fixing the parameter of interest and allowing all other parameters to float. The fixed parameter was then varied manually until the χ^2 degraded by an amount equal to two standard normal deviations as given by the χ^2 distribution. This method occasionally yields unsymmetric error bars; in favor of clarity, such error bars have been enlarged to make them symmetric (e.g., +8, −6 has been changed to ±8). Error bars were not determined for decay components with amplitudes <1%.

D. Time-Resolved Absorption Spectroscopy. Sample solutions were freshly prepared before the experiments to a final concentration of ~100 μM. Experiments were repeated on at least two samples. The samples were contained in 2 mm path length cells except for the low-temperature studies, where the path length was approximately 2.5 mm. The low-temperature measurements were made for glassed samples (*n*-butylbenzene, freezing point = 185 K)[50] contained in a copper cell with Pyrex windows clamped against indium gaskets. The cell, jacketed by a shroud, was coupled to the tip of a helium displex refrigerator and the temperature (150 ± 1 K) was feedback-controlled by a calibrated thermocouple. Lowering the temperature below 130 K led to cracking of the sample matrix.

The picosecond transient absorption (TA) apparatus is similar to systems used by other investigators.[51] A homemade linear hybrid mode-locking dye laser, which uses Rhodamine 6G and 3,3′-diethyloxadicarbocyanine iodide (DODCI) as gain medium and saturable absorber, respectively, was synchronously pumped by the second harmonic of a Coherent Antares, mode-locked Nd:YAG laser. The pumped Nd:YAG laser is coupled with a Coherent active amplitude and placement stabilization module (model 7670 AAS) and operated at 76 MHz. The dye laser was tuned to 587 ± 2 nm. The output of the dye laser was amplified to ~200 mJ in a three stage amplifier pumped by the doubled frequency of a homemade Nd:YAG Q-switched regenerative amplifier operating at 50 Hz. Amplified stimulated emission was reduced using a glass filter as a saturable absorber right after the first amplifier stage and was estimated to be ≤2% at the sample. The output of the amplifier was split into pump and probe beams. For the probe beam, 40% of the amplified pulse was focused into a continuously flowing 2 cm H_2O cell for continuum generation. A portion of the continuum probe was selected using a 400−530-nm band-pass or 590-nm long-pass filter and was then split into two beams using a pellicle beam splitter. The pump beam was directed through a motorized computer-controlled optical delay line and was aligned with one of the probe beams in a cross-configuration at the sample. All three beams were focused to a 0.2-mm diameter spot at the sample. The cross-correlation between pump and probe beams at the sample was measured by using a KDP type "C" crystal (without the continuum cell in the path) and was found to be 2 ± 0.2 ps which was the same as the background-free autocorrelation trace of the dye laser pulse. The transmitted probe beams were collimated and then latitudinally focused onto the entrance slit of a 0.2 m *f*/4 monochromator (Jarrel-Ash, Model: 82−422) coupled to a liquid-nitrogen-cooled EEV 1152 × 298 CCD detector (Princeton Instruments). Rejection of the pump beam from the spectrometer was accomplished by a second 400-530-nm band-pass or 590-nm long-pass filter placed between the sample and cylindrical lens. The polarization

(50) Barlow, A. J.; Lamb, J.; Matheson, A. J. *Proc. R. Soc. London* **1966**, *A292*, 322−342.

(51) Xie, X.; Simon, J. D. *J. Am. Chem. Soc.* **1990**, *112*, 1130−1136.

Table 1. Absorption and Fluorescence Characteristics at Room Temperature

	absorption in toluene			fluorescence yields (Φ_f)[b]			
compd	Soret (nm)	fwhm (nm)[a]		toluene	castor oil	acetone	DMSO
monomers							
TPP	420	12.0		0.11	0.12	0.14	0.14
FbU	420	12.7		0.12	0.12	0.14	0.13
FbH	420	12.4		0.11	0.12	0.14	0.13
ZnTPP	423	11.2		0.030	0.033	0.041	0.033
ZnU	423	12.9		0.035	0.038	0.050	0.038
ZnH	424	11.8		0.032	0.032	0.044	0.032
dimers							
ZnFbU	426	18.9 (13.3)	Fb em:[c]	0.13	0.15	0.14	0.050
			Zn em:[d]	≤0.0017	≤0.0056	≤0.0031	≤0.0022
ZnFbP	426	14.8 (12.4)	Fb em:	0.12	0.16	0.16	0.10
			Zn em:	≤0.0026	≤0.0047	≤0.0029	≤0.0033
ZnFbD	426	15.7 (13.6)	Fb em:	0.12	0.15	0.12	0.059
			Zn em:	≤0.003	≤0.0076	≤0.0042	≤0.0029
ZnFbB	425	13.9 (13.0)	Fb em:	0.10	0.15	0.12	0.092
			Zn em:	≤0.0048	≤0.0084	≤0.0053	≤0.0058
Zn_2U	427	18.7 (12.9)		0.043	0.045	0.054	0.053
Zn_2M	427	14.7 (12.4)		0.041	0.041	0.049	0.047
Zn_2B	426	13.6 (11.2)		0.036	0.043	0.040	0.045
trimers							
ZnZnFb	427	19.5 (17.1)	Fb em:[c]	0.12	0.14	0.14	0.095
			Zn em:[d]	≤0.0033	≤0.0076	≤0.0057	≤0.0053
Zn_3L	423,431	20.4 (12.9)		0.058	0.054	0.052	0.059

[a] Each value in parentheses shows the fwhm of the spectrum composed of the appropriate monomeric porphyrins. [b] The compounds were dissolved in CH_2Cl_2 and 2−5 μL was added to 3 mL of solvent. The emission spectra were integrated from 570 to 800 nm. The quantum yields have been corrected for the difference in solvent refractive index relative to that of toluene (except for castor oil).[45] [c] The quantum yields of the free base emission were determined with λ_{exc} in the 644−648 nm region and λ_{em} integrated from 660 to 800 nm. The integrated area was measured for the 685−800 nm region. In order to assess the total Fb porphyrin emission (620−800 nm) in the ZnFb arrays, we assume the Fb porphyrin emission has the same spectral profile in the array as in the Fb porphyrin monomers. Thus the ratio of integrated emissions in the regions 620−685 and 685−800 nm determined for the Fb porphyrin monomers in each solvent was used to compute the total Fb porphyrin emission (620−800 nm) in the ZnFb arrays, based on the integrated emission intensity of the Fb porphyrin (685−800 nm) in the array. The yield is ultimately referred to that of TPP ($\Phi_f = 0.11$).[46] [d] The quantum yields were determined with λ_{exc} in the 550−562 nm region and λ_{em} integrated from 570 to 800 nm. The extinction coefficients for the Fb and Zn components were assumed to be unchanged upon incorporation into the array. The integrated area was measured from 570 to 620 nm. In order to assess the Zn porphyrin emission (570−800 nm) in the ZnFb arrays, we assume the Zn porphyrin emission has the same spectral profile in the array as in the Zn porphyrin monomers. Thus the ratio of integrated emissions in the regions 570−620 and 620−800 nm determined for the Zn porphyrin monomers in each solvent was used to compute the total Zn porphyrin emission (570−800 nm) in the ZnFb arrays, based on the integrated emission intensity of the Zn porphyrin (570−620 nm) in the array. The yield is ultimately referred to that of ZnTPP ($\Phi_f = 0.030$).[46]

dependence of the TA data was not routinely investigated. Acquisition and analysis of time-resolved transient absorption data was controlled by software programs that translated the delay stage and averaged and ratioed the intensities from the vertically separated probe and pump plus probe images from the CCD.

III. Results

A. Dimeric Arrays. (1) Absorption Spectra. The absorption spectra of the porphyrins and arrays in toluene were measured at room temperature. The spectra of the monoethyne-substituted Fb and Zn porphyrin monomers are essentially identical to that of TPP[52] and ZnTPP,[53] respectively, with Soret bands at 420 nm (Fb) or 424 nm (Zn) and fwhm of 12 nm. The ZnFb dimers exhibit spectra that are very nearly a composite of the spectra of the component porphyrins. This is illustrated in Figure 1 which compares the absorption spectrum of ZnFbU with a composite spectrum generated by adding the spectra of ZnU and FbU. The absorptions in the visible region (Q bands, 450−700 nm) of the dimers match identically the sum of the Zn and Fb porphyrins. The Soret bands (426 nm), however, are slightly broadened with fwhm of 13.9−18.9 nm, compared with the ∼13 nm yielded by adding the spectra of the individual components. The greatest broadening of the Soret occurs for ZnFbU and the least for ZnFbB. Similarly, for the all-zinc dimers the greatest broadening occurs for Zn_2U (18.7 nm) and the least for Zn_2B (13.6 nm). The Soret band broadening may indicate significant electronic communication between the B-states of the porphyrins in the dimer. However, the bands of interest (Q bands) are virtually unchanged both in shape and in position relative to the spectra of the component parts, illustrating relatively weak electronic interaction. The Soret absorption characteristics of all the porphyrins in toluene are summarized in Table 1.

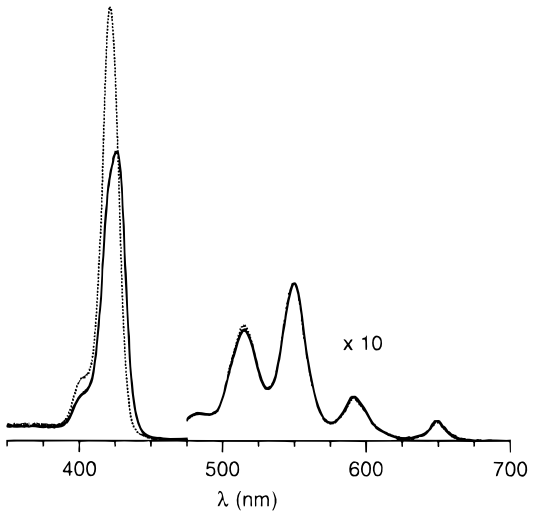

Figure 1. Absorption spectrum of ZnFbU (solid line). Composite spectrum generated by adding the spectra of ZnU and FbU (dashed line). Spectra were acquired in toluene at room temperature.

(52) Kim, J. B.; Leonard, J. J.; Longo, F. R. *J. Am. Chem. Soc.* **1972**, *94*, 3986−3992.

(53) Quimby, D. J.; Longo, F. R. *J. Am. Chem. Soc.* **1975**, *97*, 5111−5117.

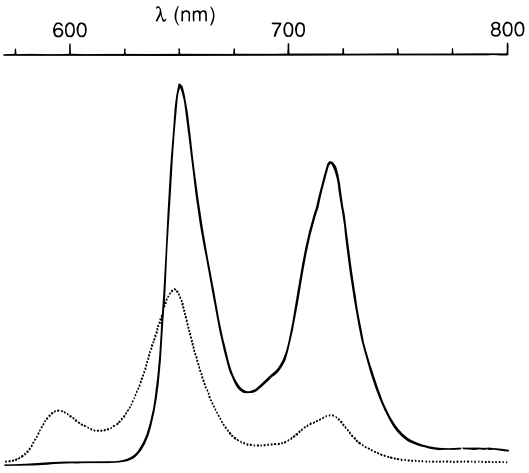

Figure 2. Emission spectrum of ZnFbU in toluene at room temperature (λ_{exc} = 550 nm) (solid line). For comparison the emission observed from an equimolar solution of the porphyrin monomers, ZnU and FbU, is shown (dotted line).

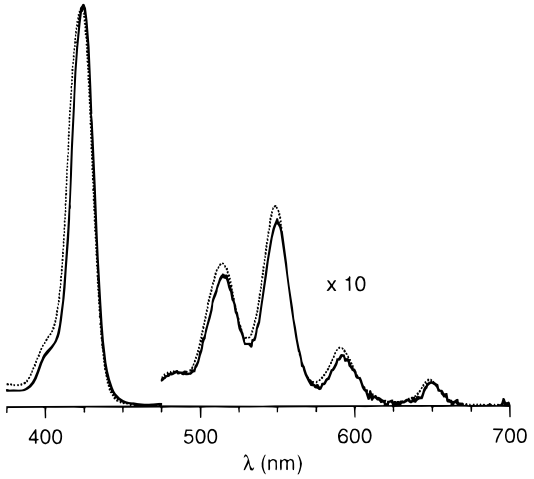

Figure 3. Excitation spectrum (λ_{em} 720 nm) (dotted line) and absorption spectrum of ZnFbU in toluene (solid line).

The absorption spectra for select compounds were also collected in a range of solvents at room temperature. The absorption maxima observed in these solvents are compiled in the previous paper.[40] In all cases, the spectra of the dimers resemble the sum of the porphyrin monomer spectra obtained in these solvents. The absorption bands of the Zn porphyrins, both as monomers and within the oligomers, shift bathochromically by up to 10 nm in going from toluene to the more polar solvents (acetone, castor oil, or DMSO). No such shift is observed for the analogous Fb porphyrins. Consequently, this result is attributed to axial ligation of Zn by the polar groups of the solvent.

(2) Fluorescence Spectra and Yields. The fluorescence emission spectra were measured for the dimers in toluene at room temperature. Illumination of ZnFbU at 648 nm, where only the Fb porphyrin absorbs, results in typical Fb porphyrin emission with quantum yield (0.13) resembling that of monomeric Fb porphyrins, including TPP. Illumination at 550 nm, where the Zn porphyrin absorbs about 4 times as intensely as the Fb porphyrin, yields emission almost exclusively from the Fb porphyrin (Figure 2). The decreased fluorescence from the Zn porphyrin is clearly shown by comparison with the emission spectrum obtained from an equimolar mixture of the porphyrin monomers, ZnU and FbU. Due to spectral overlap with the Fb porphyrin, quantitation of the amount of residual Zn porphyrin emission is difficult. Furthermore the presence of a tiny amount ($\leq$1%) of Zn porphyrin monomer in the ZnFbU sample curtails the utility of the Zn porphyrin fluorescence yield as a means of inferring the energy-transfer yield. However, the Zn porphyrin fluorescence is diminished by at least 20-fold compared with ZnU, constituting less than 1.4% of the total observed emission. The other ZnFb dimers exhibit similar results in toluene, with at least 7- to 13-fold quenching of the Zn porphyrin emission (less than 2−5% of the total emission), yet typical Fb porphyrin emission upon illumination at 550 nm. These fluorescence quantum yields are summarized in Table 1. The greatly diminished emission from the Zn porphyrin, the unaltered emission yield from the Fb porphyrin, and the predominant yield from the Fb porphyrin upon excitation of the Zn porphyrin are consistent with efficient energy transfer from the Zn to Fb porphyrin in the arrays.

The fluorescence properties of the dimers were examined as a function of solvent polarity (Table 1). Consistent with the absorption data, the emission band energies from the Zn porphyrins, both as monomers and incorporated into the arrays, are solvent dependent while those of the Fb porphyrins are not. Each of the ZnFb dimers exhibits strongly quenched Zn porphyrin emission in all solvents examined. In contrast, the fluorescence yields of the Zn porphyrin monomers are essentially constant with changes in solvent polarity. Illumination of ZnFbU at 648 nm (Fb absorption) yields typical Fb porphyrin emission in toluene, castor oil, or acetone, but the quantum yield decreases in the polar solvent DMSO to 40% of its value in toluene. The yield of emission from Fb porphyrin monomers increases slightly with increasing solvent polarity. The other ZnFb dimers also exhibit typical Fb porphyrin emission intensities in castor oil or acetone but some quenching occurs in DMSO. The most pronounced quenching (~50−60%) of the Fb porphyrin in DMSO occurs with dimers where the Zn porphyrin bears three mesityl substituents (ZnFbU and ZnFbD), with much less occurring for ZnFbP and ZnFbB. The bis-Zn dimers (Chart 3), such as Zn_2U, give a relatively constant yield of Zn porphyrin emission regardless of changes in solvent polarity.

(3) Fluorescence Excitation Spectra. The fluorescence excitation spectra of the dimers were collected in order to determine the extent to which various absorbing chromophores contribute to emission of the energy acceptor (the Fb), a common method for assessing energy-transfer efficiency.[54] The excitation spectrum of ZnFbU was obtained in toluene by scanning the excitation from 700 to 450 nm with fixed emission at 720 nm (>95% emission from the Fb porphyrin). As shown in Figure 3, an overlay of the excitation spectrum and absorption spectrum for a given array shows close matching throughout the spectrum. This indicates a high yield of singlet-state energy transfer in these compounds. In more polar solvents, including acetone and DMSO, the excitation spectra maintained the same close matching with the absorption spectra. Thus, the energy transfer does not depend on solvent polarity. The observed decreases in Fb porphyrin fluorescence yield in DMSO must reflect processes occurring after the excitation has reached the Fb porphyrin rather than those that involve the Zn porphyrin excited state.

(4) Time-Resolved Fluorescence Measurements. To investigate the excited-state dynamics, the fluorescence lifetimes of the arrays and component monomers were evaluated at several wavelengths in toluene at room temperature. The measured singlet-state lifetimes of the Zn porphyrin monomers are listed in Table 2. The presence of mesityl and *p*-ethynylaryl

(54) Haugland, R. P.; Yguerabide, J.; Stryer, L. *Proc. Natl. Acad. Sci. USA* **1969**, *63*, 23−30. Stryer, L.; Haugland, R. P. *Proc. Natl. Acad. Sci. U.S.A.* **1967**, *58*, 719−726.

Table 2. Measured Excited-State Lifetimes (ps) for the ZnFb Dimers and ZnZnFb

	toluene (298 K)[a]	toluene (298 K)[b]	DMSO (298 K)[a]	castor oil (298 K)[a]	castor oil (298 K)[b]	*n*-BB (150 K)[b,c]
ZnTPP	2040 ± 50		1930 ± 60	2200 ± 100		
ZnU	2380 ± 60		2290 ± 60	2600 ± 100		
ZnH	2260 ± 80		2080 ± 60			
ZnFbU	24 ± 7	22 ± 2	23 ± 7	34 ± 10	44 ± 2	59 ± 8
ZnFbP	48 ± 5	45 ± 7	50 ± 4		57 ± 6	
ZnFbD	40 ± 5	47 ± 5	45 ± 4		64 ± 8	
ZnFbB	90 ± 7	78 ± 10	85 ± 35		110 ± 10	
ZnZnFb	73 ± 15 (78%)	110 ± 10	54 ± 22 (78%)			
	120 ± 50 (21%)[d]		180 ± 130 (17%)[d]			

[a] Fluorescence lifetime of the Zn porphyrin measured at 600 nm. [b] TA bleach lifetime of the Fb porphyrin measured at 518 nm. [c] *n*-BB = *n*-butylbenzene. [d] A biexponential fit is required to fit these data (see text).

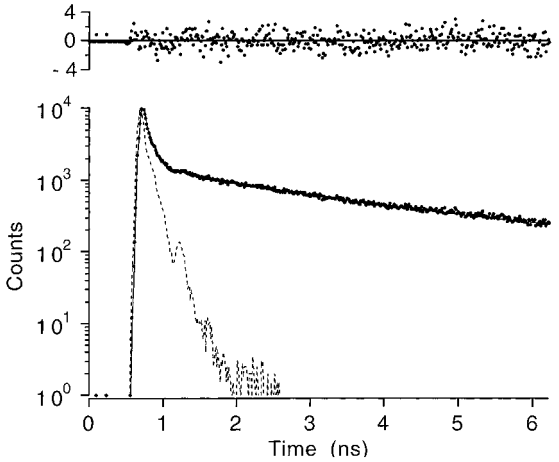

Figure 4. Emission decay curve of ZnFbU in toluene at room temperature. Data are given by the dots, the three component fit by the solid line, and the instrument response by the dashed line. The top graph gives the residuals to the fit. Excitation and emission wavelengths were 560 and 590 nm, respectively. Decay time constants of the fit are 24 ps (98%), 2 ns (1%), and 10 ns (1%).

groups at the *meso*-positions gives a slight increase in lifetime (~2.3−2.4 ns) compared with ZnTPP (2.04 ns), consistent with the observed slight increase in fluorescence yield. The slight increase in lifetime is typical for these types of porphyrins and is similar to that (2.43 ns) observed for zinc tetramesitylporphyrin (ZnTMP).

Fluorescence lifetimes of the arrays were measured using 550-nm excitation and monitoring the decay at 600 nm, where the best discrimination of the Zn porphyrin emission is afforded. For ZnFbU, a 24-ps lifetime accounts for 98% of the emission decay. This decay curve is shown in Figure 4. The remaining decay was best fit by two slower components with small amplitudes (<1% each). The exact time scales for these decays are difficult to determine due to their small amplitudes, but they roughly correspond to the Zn and Fb monomer fluorescence lifetimes (~2 and 10 ns, respectively). We believe the long decay (10 ns) originates from direct excitation of the Fb porphyrin in the dimer, while the 2 ns emission originates from a Zn porphyrin monomer impurity. This Zn porphyrin monomer is not unreacted starting material but is a trace impurity that co-chromatographs with the dimer.[40] The other dimers also yield a rapid component representing 98% of the decay and weaker slow decay components. Again, the minor, slow decay components can be fit by including two components with lifetimes similar to the Zn and Fb monomer singlet-state decays. The observed emission decay times for the Zn porphyrin in each of the dimers are summarized in Table 2. Inspection of this table makes it clear that the lifetime of the Zn porphyrin in the dimer is strongly influenced by the addition of torsionally constraining groups to the linker.

Table 3. Fluorescence Lifetimes (ns) for the Fb Porphyrins at 298 K

	toluene[a]	DMSO[b]
TPP	11.5 ± 0.8	*c*
FbU	12.6 ± 0.6	12.6 ± 0.6
FbH	12.7 ± 0.8	12.1 ± 0.6
ZnFbU[d]	12.5 ± 0.8	4.8 ± 0.4
ZnFbP[d]	10.4 ± 0.8	10.3 ± 0.8
ZnFbD[d]	10.2 ± 0.8	6.1 ± 0.4
ZnFbB[d]	12.2 ± 0.8	10.8 ± 0.8
ZnZnFb[e]	11.0 ± 0.8	9.2 ± 0.6

[a] 650 nm. [b] 646 nm. [c] Not measured. [d] The dimers exhibited a biphasic decay. The predominant lifetime (reported here) is attributed to the Fb porphyrin. A shorter lifetime (not reported) of much lower amplitude is observed and is attributed to the overlapping emission of the Zn porphyrin. [e] The trimer exhibited a triphasic decay and the predominant lifetime reported here is attributed to the Fb porphyrin.

The lifetimes of the free base porphyrins were examined at 650 nm in toluene and these values are listed in Table 3. The values for the porphyrin monomers closely resemble that of TPP. The ZnFb dimers in toluene give lifetimes essentially identical to those of the appropriate Fb monomers. One experiment was performed where the emission decay from the Fb porphyrin in ZnFbU was monitored at 725 nm. The decay is monophasic and exhibits a lifetime, $\tau = 11.3$ ns, similar to that of FbU.

The fluorescence lifetimes of the ZnFb dimers were examined in the polar solvent DMSO (Table 2). The lifetimes of the Zn porphyrins are essentially identical in toluene and DMSO, indicating the rate of energy transfer is independent of solvent polarity. The lifetimes of the Fb porphyrin monomers are unchanged in going from toluene to DMSO (Table 3). For the dimers, the Fb porphyrin lifetimes shorten by 50−60% for ZnFbU and ZnFbD, while the lifetimes of ZnFbP and ZnFbB remain unchanged in going from toluene to DMSO. These results are consistent with the 50−60% decrease in fluorescence yield observed for ZnFbU and ZnFbD in DMSO.

Castor oil, a viscous triglyceride of oleic acids, was used to investigate the possibility of solvent viscosity effects on the rates of energy transfer in the arrays. The Zn porphyrin lifetimes of select monomers and ZnFbU are listed in Table 2. For ZnFbU in castor oil at room temperature, the lifetime of the Zn porphyrin was 34 ± 10 ps while the Fb porphyrin lifetime was 12.3 ± 0.4 ns. These lifetimes are only slightly longer than those in the fluid solvent toluene and imply very little viscosity dependence on the photodynamics in this dimer.

The fluorescence lifetimes of the all-zinc arrays also were examined. These compounds exhibited a dominant decay with lifetime resembling that of a Zn porphyrin monomer. Thus the lifetimes in toluene were as follows: Zn_2U, 2.40 ± 0.08 ns (94%), 0.4 ns (6%); Zn_3L, 2.35 ± 0.08 ns (93%), 0.3 ns (7%). The lifetimes in DMSO were similar: Zn_2U, 2.24 ± 0.08 ns (88%), 0.1 ns (12%); Zn_3L, 2.17 ± 0.08 ns (84%), 0.1 ns (16%).

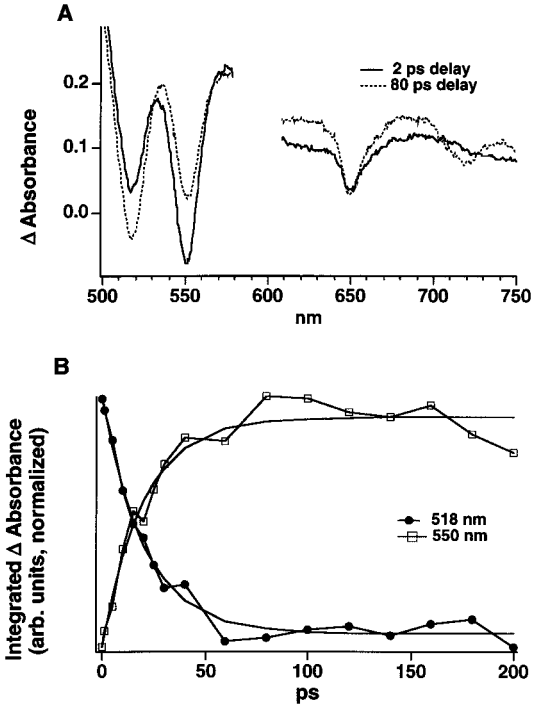

Figure 5. (A) Transient absorption data for ZnFbU in toluene at room temperature at 2 (—) and 80 (- - -) ps delay. (B) Kinetic trace of ZnFbU in toluene at room temperature showing the recovery of the Zn porphyrin ground state (550 nm) and the bleaching of the Fb porphyrin (518 nm).

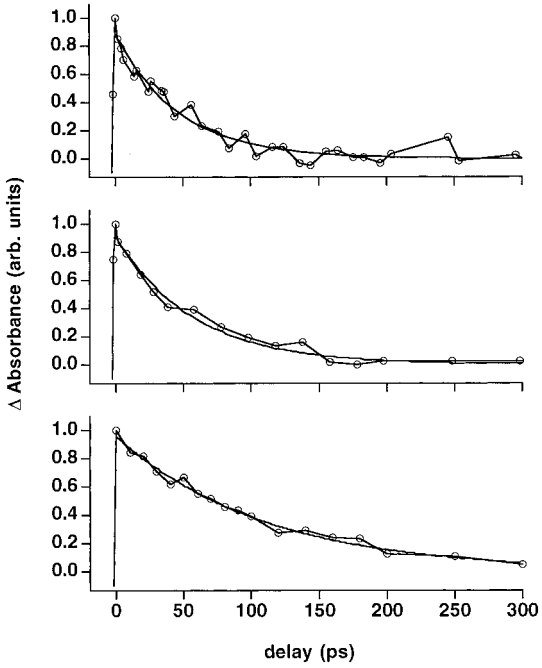

Figure 6. Kinetic traces of absorption changes for selected arrays at room temperature. The integrated intensity data (circles) are plotted for a 15 nm window centered on the primary Fb porphyrin bleach component at 518 nm as a function of pump/probe delay. A single exponential fit is superimposed. The top trace is for ZnFbP in toluene. The middle trace is for ZnFbP in castor oil, and the bottom trace is for ZnZnFb in toluene.

The origin of the biphasic decays in these compounds is not known and will be the subject of further investigation.

(5) Time-Resolved Absorption Measurements. Time-resolved absorption (TA) data were obtained for the arrays dissolved in toluene at room temperature. Examples of TA spectra acquired for ZnFbU at 2 and 80 ps delay (solid and dashed line, respectively) are shown in Figure 5A. Roughly one third of the incident energy at the pump wavelength of the TA experiment (587 nm) is absorbed by the Zn porphyrin in all of the dimers. The singlet-excited-state absorption profiles of both the Zn and Fb porphyrins are broad and not readily distinguishable. However, the TA experiments allow identification of the transient states by examination of the associated ground-state bleach accompanied by investigation of the near-infrared region.[55] The appearance of a relatively intense bleach band near 550 nm indicates an excited state associated with the Zn porphyrin at 2-ps delay. Longer delay times reveal increasingly intense bleaching at 518 nm associated with the ground-state Q-band absorption of the Fb chromophore. As shown in Figure 5A, the near-infrared region of the TA data exhibits stimulated emission from the Zn porphyrin (Q(0,0)) at 650 nm at early delay times while Fb emission is observed at 720 and 650 nm (Q(0,1) and Q(0,0), respectively) at longer delays. No additional features attributable to charge transfer or triplet states are indicated by the data. In general, the TA data from the arrays in toluene indicate that the only states populated on the picosecond time scale are the singlet excited states of the Zn and Fb porphyrins. Thus, like the fluorescence excitation spectra, the TA data indicate that energy transfer to the Fb porphyrin is the predominant decay channel for the Zn porphyrin excited state in the arrays.

The dynamics of energy transfer in the arrays were evaluated by determining the time dependence of the cumulative absorption change over a roughly 15-nm window centered at the Fb porphyrin bleach band at 518 nm. Using this approach, the sudden onset of absorption associated with the singlet excited state(s) provides a measure of zero time delay and the effects of chirping (wavelength-dependent temporal dispersion) can be ignored. Although both the Zn and Fb porphyrins absorb (1:9) in the monitored wavelength region, the rate of spectral evolution observed for the dimeric arrays will not depend upon the overlapped features if energy transfer is the only significant photophysical process and if the signal from the directly excited Fb porphyrin is static over the time period of interest. Thus, the kinetics observed at 518 nm will give the energy-transfer rates even though the absorption bands of the ground and excited states overlap at this wavelength. Similarly, at 550 nm the Zn porphyrin absorbs roughly 4.5 times more than the Fb porphyrin and the rate of recovery of this absorption band should complement the increased bleach observed at 518 nm for the energy-transfer process. Indeed, as shown in Figure 5B, a plot of transient absorption changes at 518 and 550 nm over the initial 200 ps of the reaction shows the rate of bleach at 518 nm matches the recovery at 550 nm. The kinetic traces at 518 and 550 nm were well-fit by single exponentials with a time constant of 22 ps. In general, single exponential behavior is observed (within error) for the evolution of all of the TA data described in this paper. Three selected examples of the temporal development of the 518 nm bleach, with superimposed single exponential decay fits, are shown in Figure 6. The temporal evolution of the Fb absorption bleach in ZnFbU as well as ZnFbP, ZnFbD, and ZnFbB is included in Table 2 (column 2). The mono-hindered dimers exhibit ~2-fold slower rates compared with ZnFbU, while the lifetime of ZnFbB is longer still than those of the mono-hindered systems.

TA data were also acquired for the dimers dissolved in castor oil. The TA features observed for the dimers in this solvent

(55) (a) Rodriguez, J.; Kirmaier, C.; Holten, D. *J. Am. Chem. Soc.* **1989**, *111*, 6500−6506. (b) Rodriguez, J.; Kirmaier, C.; Holten, D. *J. Chem. Phys.* **1991**, *94*, 6020−6029.

(56) Scholes, G. D.; Ghiggino, K. P.; Oliver, A. M.; Paddon-Row, M. N. *J. Phys. Chem.* **1993**, *97*, 11871−11876.

are similar to those obtained with toluene. Single exponential fits of the bleaching at 518 nm (Figure 6, middle trace) gave lifetimes that were slowed by ~1.3- to 2-fold compared with those in toluene. These lifetimes are included in Table 2.

TA data were acquired for ZnFbU and ZnFbB as a function of temperature. The samples were held at 150 K in *n*-butylbenzene, which is similar to toluene in its solvation properties but forms a superior glass upon freezing. At room temperature, the TA lifetimes observed for each of these arrays are identical, within error, to those observed in toluene. Low-temperature data (Table 2) qualitatively suggest that the energy-transfer rates decrease slightly as the temperature is lowered. However, the quality of the TA spectra is relatively poor (due in part to the reduced transmission associated with the low-temperature cell), and a temperature dependence was not conclusively demonstrated for the photodynamics of ZnFbB.

B. A Trimeric Array. The ZnZnFb trimer (Chart 3) comprised of two Zn porphyrins and one Fb porphyrin in a linear array is of interest because the two Zn pigments are approximately isoenergetic. Analysis of this system provides an opportunity to measure the rate of energy migration between the two Zn porphyrins, which will figure prominently in the dynamics of multiporphyrin arrays such as the molecular wire, a linear array comprised of a boron−dipyrromethene, three consecutive Zn porphyrins, and a terminating Fb porphyrin.[23] Within the ZnZnFb trimer, the Zn/Fb linkage is analogous to that of ZnFbP while the Zn/Zn porphyrin linkage is analogous to that of Zn_2U.

The absorption spectrum of the trimer in toluene (not shown) shows broadening and slight splitting of the Soret band (fwhm 19.5 nm; expected 17.1 nm based on component parts) but the visible bands identically match the sum of the spectra of the component parts. Illumination at 648 nm, where only the Fb porphyrin absorbs, results in typical Fb porphyrin emission with quantum yield (0.12) resembling that of monomeric Fb porphyrins. Illumination at 550 nm, where the Zn porphyrins absorb 9 times more than the Fb porphyrin, yields emission predominantly from the Fb porphyrin. As in the case of the dimers, quantitation of the amount of residual Zn porphyrin emission is difficult as the emission bands of the Zn and Fb porphyrins overlap. However, the emission from the Zn porphyrin is diminished by at least 9-fold and thus, the Zn porphyrin emission constitutes less than 3% of the total emission. These fluorescence quantum yields are summarized in Table 1.

The dynamics of energy migration in ZnZnFb were probed by time-resolved fluorescence and absorption spectroscopies. The fluorescence decay at 600 nm (550 nm excitation), representing both Zn porphyrins, is well fit with two short lifetimes ($\tau \sim 73$ and 120 ps) which together account for 99% of the amplitude (78 and 21%, respectively). Using only one lifetime ($\tau \sim 87 \pm 18$ ps) allows an approximate fit of the fluorescence decay. As is the case for the dimeric arrays, two long lifetime components (2 and 10 ns) with less than 1% amplitude each are required to fit the data; the former is due to an impurity and the latter is due to direct excitation of the Fb porphyrin in the trimer. In contrast, the Fb porphyrin bleach in the TA data exhibits a monophasic decay ($\tau \sim 110$ ps; Figure 6, bottom trace). A plot of the logarithm of the change in absorbance versus time revealed no obvious inflection points even though energy transfer would not be expected to evolve as a first-order process. The Fb porphyrin in ZnZnFb gives a typical Fb porphyrin fluorescence decay (11.0 ns) in toluene. The results of the studies of ZnZnFb are included in Tables 2 and 3.

IV. Discussion

There are four striking features of the photodynamic behavior of the diarylethyne-linked arrays: (1) The arrays exhibit high yields of energy transfer in spite of the weak coupling between adjacent porphyrins. (2) The arrays display systematic variation in energy-transfer rates upon structural alterations of the diarylethyne linker. (3) The rate of energy transfer from Zn to Fb porphyrins is hardly affected (≤2.5-fold) by changes in solvent polarity, viscosity, or temperature. (4) The fluorescence yield from the Fb porphyrin in the ZnFb arrays is like that of Fb porphyrin monomers in toluene, castor oil, or acetone, but decreases in the very polar solvent DMSO, in contrast to the solvent-independent fluorescence yield of the all-zinc porphyrin arrays. Each of these results has a critical bearing on the goal of rational design of efficient, controlled energy-transfer systems. The discussion of the photodynamic behavior in the arrays is structured as follows. First, we examine the behavior of the arrays in toluene where energy transfer dominates the early time photodynamics. In this discussion, we consider both the efficiency and mechanism of energy transfer and how torsional constraints in the linker influence mechanism. We then discuss the effects of environmental factors, including solvent and temperature, on the photodynamics. Finally, we examine energy transfer in the trimers and its implication for the behavior of extended linear arrays similar to the molecular wire.

A. Energy Transfer in Dimeric Arrays. (1) Efficiencies and Rates. The fluorescence yield, fluorescence excitation, transient absorption, and fluorescence lifetime studies all indicate that the yield of energy transfer is well over 90% for all the ZnFb dimers. A precise determination of the efficiency (Φ_{trans}) can be obtained by several methods. Fluorescence quantum yield measurements, including careful comparison of the static absorption and fluorescence excitation spectra, provide a direct measure of the efficiency. Alternatively, comparison of the rates of energy transfer with those of competitive decay channels allows an inference of the efficiency. The latter method has been used to estimate the energy-transfer efficiency for the arrays because the yield is high, the fluorescence spectra of Zn and Fb porphyrins overlap significantly, the Zn porphyrin is intrinsically ~3 times less emissive than the Fb porphyrin, and a residual amount (≤1%) of Zn porphyrin monomer is present in all of the samples. Together, these factors render precise determination of the energy-transfer efficiencies in the arrays unreliable by static measurements.

The decay channels competing with energy transfer include internal conversion (ic), intersystem crossing (isc), and emission (rad). Owing to the weak coupling between the porphyrins in the arrays, these channels should exhibit nearly the same rates that occur in monomeric porphyrins. This important property of the arrays is evidenced by the lack of any apparent triplet-state transient absorption (isc) and the similarity between the emission band shapes of the arrays and those of monomers (rad). Further support is provided by the observation that the relative fluorescence yields of the Fb porphyrin in dimers (as measured statically for ZnFbU) are not significantly different from that of TPP (ic, isc, rad). Finally, the observed fluorescence lifetimes of zinc arylethyne-substituted porphyrin monomers are comparable to those of ZnTPP and ZnTMP which indicates that the presence of additional vibrational coordinates in the linker does not substantively perturb the basic photophysics of the porphyrin (ic, isc, rad). Any small changes that do occur are insignificant relative to the very rapid rate of energy transfer. The general retention of monomer-like behavior for many properties of the diarylethyne-linked arrays can be contrasted with the behavior of oligomers comprised of porphyrins directly

Table 4. Energy-Transfer Rates and Efficiencies for the ZnFb Dimers[a,b]

	ZnFbU			ZnFbP[c]		ZnFbD[c]		ZnFbB		
	toluene[d] (298 K)	castor oil (298 K)	*n*-BB[e] (150 K)	toluene[d] (298 K)	castor oil (298 K)	toluene[d] (298 K)	castor oil (298 K)	toluene[d] (298 K)	castor oil (298 K)	*n*-BB[e] (150K)
k_{trans}^{-1}	24	45	60	48	58	45	66	88	115	91
Φ_{trans}	0.99	0.98	0.98	0.98	0.98	0.98	0.97	0.96	0.95	0.96
k_{TB}^{-1}	25	48	65	51	63	48	73	100	137	104
χ_{TB}	0.96	0.94	0.92	0.93	0.92	0.94	0.91	0.88	0.84	0.87
χ_{TS}	0.04	0.06	0.08	0.07	0.08	0.06	0.09	0.12	0.16	0.13

[a] For comparison with the lifetimes (Table 2) the reciprocals of the rates (k_{trans}^{-1} and k_{TB}^{-1}) in ps are listed. [b] The overall energy transfer rates and efficiencies were calculated from eqs 3 and 4 using $\tau_D = 2.4$ ns. The through-bond rates and efficiencies were calculated from eqs 5 and 6 assuming that the through-space rate is a constant (720 ps)$^{-1}$ (Appendix). [c] Low-temperature measurements were not made on ZnFbP and ZnFbD. [d] Based on the average of the lifetimes obtained from the fluorescence and TA measurements (Table 2). [e] *n*-BB = *n*-butylbenzene.

linked by ethyne or butadiyne groups at the *meso*-carbon atoms of the ring.[30−39] This type of linkage promotes strong electronic coupling which renders the intrinsic photophysics of the constituent porphyrins quite different from that of monomers.

The weak electronic coupling between the diarylethyne-linked porphyrins permits the energy-transfer rates (k_{trans}) and efficiencies (Φ_{trans}) to be estimated from the measured rates of the fluorescence decay of the Zn porphyrin within the dimers (τ_{DA}) and that of the appropriate Zn porphyrin monomer (τ_D) using the formulae:

$$1/\tau_D = k_{rad} + k_{isc} + k_{ic} \quad (1)$$

$$1/\tau_{DA} = k_{rad} + k_{isc} + k_{ic} + k_{trans} \quad (2)$$

$$k_{trans} = 1/\tau_{DA} - 1/\tau_D \quad (3)$$

$$\Phi_{trans} = k_{trans}\tau_{DA} = 1 - \tau_{DA}/\tau_D \quad (4)$$

For reasons discussed later, deactivation of the energy donor excited state in the dimer by charge transfer is not included. Regardless, charge-transfer processes are not significant contributors to the photodynamics of the arrays in toluene. Furthermore, the yield of reverse energy transfer (from the Fb porphyrin to the Zn porphyrin) is negligible due to the energy difference of the respective excited states. The excited-state lifetimes obtained for the dimers by fluorescence and TA measurements are in close agreement (Table 2). Consequently, the average of these two measurements is used as the value of τ_{DA}; the measured value of τ_D is ∼2.4 ns. Using these values, the k_{trans} values in toluene at room temperature are calculated to be (24 ps)$^{-1}$ (ZnFbU), (48 ps)$^{-1}$ (ZnFbP), (45 ps)$^{-1}$ (ZnFbD), and (88 ps)$^{-1}$ (ZnFbB). The corresponding Φ_{trans} values are 99% (ZnFbU), 98% (ZnFbP and ZnFbD), and 96% (ZnFbB). The values of k_{trans} and Φ_{trans} are summarized in Table 4. It should be noted that an assessment of the Zn porphyrin emission yield in the dimers based on the assignment of the 600 nm emission entirely to the Zn porphyrin gives a quenching of approximately 6- to 20-fold (by static measurements), whereas the quenching indicated by the lifetime measurements ranges from 25-fold (ZnFbB) to 90-fold (ZnFbU). These disparities reflect the fact that the residual Zn porphyrin emission is too weak to be reliably measured in the presence of the large overlapping emission of the Fb porphyrin in the dimers.

(2) Mechanisms and Structural Control. The energy transfer in the diarylethyne-linked arrays could proceed by through-bond[56] and/or through-space (Förster)[57] mechanisms. Two observations indicate that a through-bond process is the dominant mechanism for all the ZnFb dimers. First, the energy-transfer rates for all the dimers are too fast to be consistent with a through-space mechanism. Using the point-dipole approximation, the through-space energy-transfer rate for the dimers is estimated to be ∼(720 ps)$^{-1}$ (Appendix). Refinement of this calculation using point monopoles can shorten the calculated energy-transfer rates,[58] but not to the extent required for consistency with the data. Second, the addition of torsional constraints to the linker would not be expected to strongly influence a through-space energy-transfer process (Appendix). Contrary to this prediction, the observed excited-state photodynamics are significantly affected by torsional constraints. Thus, through-bond energy transfer is an essential feature of the photodynamics of the diarylethyne-linked arrays.

While a through-bond mechanism is implicated as the principal contributor to the energy-transfer process in the arrays, the through-space mechanism should still participate. If the observed energy-transfer rates (k_{trans}) are assumed to be due to the additive effects of through-bond (k_{TB}) and through-space (k_{TS}) processes (eq 5), then the fractional amounts of through-bond contribution (χ_{TB}) and through-space contribution (χ_{TS}) can be estimated (eqs 6 and 7).

$$k_{trans} = k_{TB} + k_{TS} \quad (5)$$

$$\chi_{TB} = k_{TB}/k_{trans} \quad (6)$$

$$\chi_{TB} + \chi_{TS} = 1 \quad (7)$$

Using the k_{trans} values listed in Table 4 and $k_{TS} = (720\ ps)^{-1}$, the k_{TB} values are determined to be (25 ps)$^{-1}$ (ZnFbU), (51 ps)$^{-1}$ (ZnFbP), (48 ps)$^{-1}$ (ZnFbD), and (100 ps)$^{-1}$ (ZnFbB). The corresponding χ_{TB} values are 96% (ZnFbU), ∼93% (ZnFbP and ZnFbD), and 88% (ZnFbB). The values of k_{TB} and χ_{TB} are included in Table 4. Accordingly, the addition of torsional constraints to the linker progressively decreases the through-bond energy-transfer rates in a more dramatic fashion than indicated by the observed decays, suggesting that the dihedral angle between the porphyrin and aryl rings in the linker is the critical structural feature which mediates this mechanism. Only for ZnFbB does the through-space mechanism make more than a 10% contribution to the overall energy-transfer rate (Table 4).

There are two distinct types of motions that can occur in the dimers involving the two porphyrins and their adjacent aryl groups in the linker: (1) The two porphyrins can rotate freely with respect to each other about the cylindrically-symmetric ethyne bond, while the respective porphyrin−aryl group dihedral angles remain fixed. (2) An aryl group of the linker can rotate toward coplanarity with the adjacent porphyrin, while maintaining a fixed porphyrin−porphyrin dihedral angle. The molecules in fluid solution are expected to sample a wide variety of geometries via combinations of these motions. In terms of energy transfer, rotation of the porphyrins is expected to cause only a 25% change in the rate of through-space energy transfer, with the maximum for coplanar porphyrins and the minimum

(57) Förster, Th. *Ann. Phys.* **1948**, *2*, 55−75.

(58) Chang, J. C. *J. Chem. Phys.* **1977**, *67*, 3901−3909.

for perpendicular porphyrin planes (Appendix). For porphyrin−porphyrin through-space energy transfer, the porphyrin−aryl group dihedral angle is expected to be irrelevant. For through-bond energy transfer, the effect of porphyrin−porphyrin dihedral angle is not known. However, the attainable porphyrin-aryl dihedral angle appears to have a significant influence on the rate of energy transfer in the four ZnFb dimers. In addition to these rotational motions, the linker also slightly bends[41] though these motions are considered to be essentially the same for all four dimers.

The effect of torsional constraints on the energy-transfer rates suggests that the through-bond electronic coupling is mediated by the π-electron system of the linker. In this view, the decrease in the energy-transfer rate which occurs upon addition of torsional constraints can be attributed to the diminished propensity of the porphyrin and aryl rings in the linker to approach coplanarity. This view is also consistent with resonance Raman data previously reported[42] and in a companion paper.[43] The relative decrease in the through-bond energy-transfer rate which occurs upon going from the mono-hindered to bis-hindered dimers (50 to 100 ps)$^{-1}$ versus the unhindered to mono-hindered systems (25 to ∼50 ps)$^{-1}$ shows that the effects of torsional constraints on the through-bond energy-transfer rates are not simply additive. Indeed, the probability distribution for sampling torsional angles which permit efficient energy transfer in a bis-hindered system might be expected to be approximately the product of the distribution functions which describe a mono-hindered system. While the effects associated with the torsional constraints seem consistent with conjugation of the linker and porphyrin π-systems, the extent of the participation of the linker in the excited-state electronic structure remains poorly defined. This is so because the extent of conjugation depends not only on π overlap (as determined by the torsional angle) but also on the relative energies of the orbitals in the porphyrin, aryl linker, and ethyne bridge. The energies (and identities) of all the important orbitals are not known with certainty. Regardless, the fact that addition of the ethyne linker does not have a significant effect on the absorption spectrum indicates that the extent of conjugative stabilization is relatively small. In order to directly probe the excited-state structure, we are currently pursuing time-resolved resonance Raman experiments specifically aimed at examining the effects of torsional constraints on the vibrational frequencies of the diarylethyne linkers.

There have been a number of other studies of energy transfer in ZnFb porphyrin dimers with varying linker structures.[4−29] These linkers encompass both saturated and unsaturated systems of different lengths and degrees of flexibility. Energy-transfer rates nearly as fast as some of those reported herein have been observed, including (43 ps)$^{-1}$ in a phenyl−amide−phenyl-linked ZnFb dimer[17] which has the same number of bonds as the diarylethyne linkers. Slower rates have been measured by Osuka *et al.* in dimers containing *meso*-linkers with alkyl substituents at the flanking β-pyrrole positions, including (227 ps)$^{-1}$ in a bis-spiroindane linked ZnFb dimer,[15] (128 ps)$^{-1}$ in a biphenyl-linked ZnFb dimer,[15] and (322 ps)$^{-1}$ in an unhindered diphenylethyne linked ZnFb dimer.[28] The energy-transfer processes in these systems have been modeled by both Förster and Dexter mechanisms. The slower rates in all of the β-pyrrole substituted dimers compared with the dimers presented here are quite surprising. Indeed, the biphenyl linker provides a pathway two bonds shorter than the diarylethyne yet is slower than any of our dimers. The diphenylethyne linker is identical to that in our ZnFbU (24 ps)$^{-1}$ yet the rate is 13 times slower. The origins of the discrepancy between the energy-transfer rates measured for our arrays versus those of Osuka and co-workers are not obvious given the similarity in the overall structure of the two types of arrays.

(3) Effects of Solvent and Temperature. The relatively high solubility of the arrays in a variety of solvents allows for in-depth studies of how the medium influences the photodynamics. The most striking observation is that change in the viscosity, temperature, or polarity of the medium has a relatively small effect, altering the energy-transfer rates by a factor of ≤2.5-fold. Such small changes are of little importance for the dimers, causing net efficiency changes of ∼1%, but would become relevant when manifest in a multiplicative fashion in large multiporphyrin arrays. We consider these medium effects in turn: (1) In the viscous medium castor oil, the excited-state lifetimes and resulting energy-transfer rates are 1.3−1.9 times slower as compared with toluene (Tables 2 and 4). One interpretation is that higher viscosity could restrict the torsional motions of the aryl rings of the linker and hence alter the through-bond electronic communication between the porphyrin and the macrocycle. Assuming the rate of through-space energy transfer is independent of viscosity (Appendix), the through-bond energy-transfer rates in castor oil calculated using eq 5 are ∼(48 ps)$^{-1}$ (ZnFbU), ∼(68 ps)$^{-1}$ (ZnFbD and ZnFb), and ∼(137 ps)$^{-1}$ (ZnFbB). The largest change occurs for ZnFbB, where the fraction of through-bond transfer χ_{TB} decreases from 88% to 84% in going from toluene to castor oil. The validity of this interpretation is not clear, as excited-state torsional motions have been characterized as viscosity independent for some compounds and viscosity dependent for others.[59−61] (2) At low temperature (150 K), the rates of energy transfer only slightly decrease (≤2.5 fold). The rate observed in ZnFbU slows 2.5-fold (from (24 ps)$^{-1}$ to (60 ps)$^{-1}$), while no change is observed within experimental error for ZnFbB. This observation suggests that freezing the solvent either restricts the ability of the aryl group to sample "good" geometries (i.e., tending toward greater coplanarity with the porphyrin) or perhaps that the change in temperature leads to a change in the average dihedral angle between the linker and porphyrin. The latter could arise if the torsional coordinate is a large-amplitude, low-frequency, highly anharmonic mode with an average geometry that is statistically influenced by temperature. Temperature-induced conformational changes would be expected to be greater in ZnFbU than ZnFbB because the absence of torsional constraints in the former dimer affords access to a wider range of dihedral angles. (3) Solvent polarity appears to have little effect on energy-transfer efficiencies as measured by fluorescence excitation spectra or by Zn porphyrin emission quantum yields, which are essentially unchanged in toluene and the polar solvents acetone and DMSO. The fluorescence lifetimes of the Zn porphyrin in the ZnFb dimers are essentially unchanged in toluene and DMSO. In summary, the absence of any marked perturbation of the energy-transfer rates by changes in solvent polarity, viscosity, or temperature indicates that these arrays could be incorporated in solid matrices or thin films with little expected change in performance.

Polar solvents do have one significant effect on the fluorescence properties of some of the arrays. The emission intensity from the Fb component of ZnFbU and ZnFbD is significantly decreased in the polar DMSO. This type of solvent dependence is not observed for monomeric Fb porphyrins, monomeric Zn porphyrins, or any all-zinc porphyrin containing arrays (Zn_2U, Zn_2M, Zn_2B, Zn_3L, Table 1). The Fb porphyrin fluorescence

(59) Loufty, R. O.; Arnold, B. A. *J. Phys. Chem.* **1982**, *86*, 4205−4211.
(60) Ben-Amotz, D.; Harris, C. B. *Chem. Phys. Lett.* **1985**, *119*, 305−311.
(61) Simon, J. D.; Su, S-G. *J. Phys. Chem.* **1990**, *94*, 3656−3660.

yield and lifetime correspond very closely. Indeed, 62% quenching is observed for ZnFbU and the lifetime is shortened by 62% to 4.8 ns (compared with FbU), and 56% quenching is observed for ZnFbD and the lifetime is shortened by 50% to 6.1 ns (compared with FbH). Much less quenching or shortening of the free base lifetime is observed in ZnFbP and ZnFbB. The quenching observed for the Fb porphyrin in ZnFbU and ZnFbD in DMSO is consistent with an interporphyrin charge-transfer process. This pathway for electronic interaction is effectively closed in solvents such as toluene, castor oil, or acetone ($\epsilon = 20.7$), emerging only in the very polar solvent DMSO ($\epsilon = 46.7$). Our evidence for interporphyrin charge transfer is tenuous, however, such a phenomenon has been observed in ZnFb dimers by Gust *et al.*[17] The presence of charge transfer in ZnFbU and ZnFbD, with significantly lesser amounts in ZnFbP and ZnFbB, may be due to a driving force effect. In the former pair of arrays the Zn porphyrin is substituted with three mesityl groups, while in the latter the Zn porphyrin bears three phenyl groups. It must be emphasized that the charge-transfer process occurs *after* the excitation reaches the Fb porphyrin and does not appreciably influence the energy transfer between the Zn and Fb porphyrins in the array. Accordingly, inclusion of a charge-transfer rate in eq 2 is not necessary.

B. Energy-Transfer Dynamics in a Trimeric Array. The photodynamics which occur in the ZnZnFb array presumably include reversible energy transfer between the approximately isoenergetic Zn porphyrins. The rate of this process is of general interest because adjacent Zn chromophores are an intrinsic component of extended arrays such as the molecular photonic wire.[23] A few reasonable assumptions permit numerical modeling of the time-resolved spectroscopic behavior of the trimer. These are as follows: (1) The absorption characteristics of the two Zn chromophores are identical. Accordingly, the initial excitation is distributed equally between these two porphyrins. (2) Two-photon absorption by the array is negligible under the conditions of these time-resolved measurements. (3) The energy-transfer rate from the terminal to the central Zn porphyrin (k_1) is equal to the reverse rate (k_{-1}). (4) The energy-transfer rate between the central Zn and the Fb porphyrins (k_2) is equal to that measured for the analogous dimer, ZnFbP. This model is illustrated in Scheme 1, and was evaluated numerically by adjusting k_1 in attempts to fit the Fb porphyrin bleach (TA data) or the combined Zn porphyrin singlet-state decay (fluorescence data). These calculations indicate that Scheme 1 can successfully reproduce the observed transient data.

The coupled differential equations describing the temporal evolution of the energy transfer between the various chromophores are modeled by fixing the rates and solving for the concentrations of the singlet excited states of each of the three individual chromophores every 0.5 ps following $t = 0$. The resulting decay curves are then fit by a single-exponential expression. The inherent decay of the Zn porphyrin singlet excited states via the characteristic 2.4-ns lifetime is included in the calculation, which was found to accurately reproduce the excited state decay behavior for the dimers.

To model the TA data, the contribution of each chromophore to the changes in absorption was weighted by its extinction coefficient at this wavelength. With a k_2 value of $(48\ \text{ps})^{-1}$ (Table 4), a k_1 value of $(52\ \text{ps})^{-1}$ yields a close fit with the observed 110 ps bleaching decay of the Fb porphyrin. The value of k_2 was varied between $(42\ \text{ps})^{-1}$ and $(52\ \text{ps})^{-1}$ in order to approximately explore the error limits on this parameter (Table 4). Over this range of k_2 values, the 110-ps lifetime dictates that k_1 range from $(33\ \text{ps})^{-1}$ to $(71\ \text{ps})^{-1}$. As the values of k_1 and k_2 become more disparate, the quality of the single exponential fit degrades, although at what point loss of single exponential behavior would be apparent in the TA measurement is not obvious due to the S/N of the data. A general observation is that the model yields approximate first-order production of the Fb singlet excited state when $k_1 \geq k_2$. True pseudo-first-order behavior is found for $k_1 \gg k_2$ ($k_1 > (10\ \text{ps})^{-1}$); however, this regime dictates that the Fb population accumulates with an 87-ps risetime, which is somewhat outside the range of the TA data. Thus the most reasonable rate constants that fit the TA data are $k_2 = (47 \pm 5\ \text{ps})^{-1}$ and $k_1 = k_{-1} = (52 \pm 19\ \text{ps})^{-1}$.

Scheme 1. Kinetic Model for Energy Transfer among Porphyrins in ZnZnFb Trimer

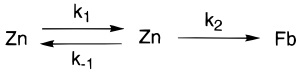

The combined Zn porphyrin fluorescence decay at 600 nm also can be approximately fit by a single exponential with a lifetime of 87 ± 18 ps, though a better fit is obtained with a biexponential expression (73 ps (78%), 120 ps (21%)). However, this 87 ps lifetime is faster than that obtained from the analysis of the TA data. As noted above, such a rapid decay of the Zn porphyrin singlet states within the trimer can only be readily modeled within Scheme 1 if k_1 is assumed to be greater than $(10\ \text{ps})^{-1}$. Whether or not such a rate is reasonable will be the subject for a future investigation.

V. Summary

High yields (>95%) of energy transfer, a sine qua non of light-harvesting, are achieved in synthetic porphyrin arrays built with diarylethyne linkers. These arrays achieve efficient energy transfer without close contact of the porphyrins (20-Å separation). In addition, the arrays exhibit excellent photostability and high solubility. These properties enable in-depth studies of the photophysical properties of the arrays under a wide variety of conditions (photon flux, solvent, temperature). Photostability and high solubility are also essential material properties for the construction of prototypical photonic devices based on the diarylethyne-linked porphyrin motif.

The rates of energy transfer in the diarylethyne-linked arrays depend in a systematic manner on the structure of the linker. Both the structural and temperature dependencies of the energy-transfer kinetics reveal that there are many conformations that will permit energy transfer, albeit at varying rates. Assuming that a torsional coordinate mediates the through-bond component of this process, it is certain that the period of the vibration is such that all geometries capable of energy transfer are dynamically averaged during the process. Thus, the single exponential lifetimes originate from a variety of geometries. Further, the observed single-exponential decays are likely comprised of both through-space and through-bond processes. Control of the degree of inter-porphyrin communication by structural factors has been demonstrated. The yield of emission from the Fb porphyrin remains like that of a Fb porphyrin monomer in the media of toluene, castor oil, or acetone. Charge transfer from the Fb to the Zn porphyrin appears in the polar solvent DMSO, but the energy transfer from the Zn to the Fb is not obviously influenced by such changes. Nevertheless, the charge-transfer-induced fluorescence quenching observed in DMSO indicates that the diarylethyne linkers can support rapid photoinduced electron transfer. Structural designs that take advantage of these electron-transfer reactions are under consideration.

The diarylethyne-linked arrays also support efficient energy migration among isoenergetic pigments. The energy-transfer

rates between two adjacent Zn porphyrins are comparable to those observed between a Zn/Fb pair. Isoenergetic energy transfer is an essential phenomenon in natural light-harvesting systems. However, in light-harvesting proteins, the pigments are not covalently linked and the mechanism of energy transfer is through-space. Nevertheless, the energy-transfer rates in the natural systems are extraordinarily fast, with typical values in the range of $(0.1\ \text{ps})^{-1}$ to $(1\ \text{ps})^{-1}$.[1,62] While the rates in the diarylethyne-linked synthetic arrays are 20 to 1000 times slower, they are still such that energy transfer is the predominant excited-state process. The predominance of through-bond communication in the synthetic arrays provides greater versatility in controlling the energy-transfer rates by using structural alterations. These alterations afford the possibility of tuning the rates and the spatial direction of energy flow.

Finally, the results reported herein indicate that diarylethyne-linked porphyrin arrays can be designed with predictable energy-transfer properties. The design and construction of extended arrays with numerous porphyrins should be relatively straightforward. The negligible effects due to environment (solvent polarity, viscosity, temperature) indicate that the arrays should function efficiently if embedded in solid matrices or supported in thin films. Prototypical extended arrays, such as the molecular photonic wire[23] and optoelectronic gates,[29] have already been constructed. These architectures, as well as the smaller dimers and trimer studied here, use Fb porphyrins as the low energy trap. However, it should be emphasized that the use of a Fb porphyrin as the trap is merely a convenience and other types of traps could be incorporated into the arrays. For example, traps could be designed to exhibit better spectral distinction or significantly reduced charge-transfer properties. These, and other approaches, will augment our ongoing effort aimed at the rational design of synthetic light-harvesting systems and molecular photonic devices.

Acknowledgment. This work was supported by the LACOR Program (D.F.B) and Subcontract No. 346KK014-19C (J.S.L.) from Los Alamos National Laboratory, grants GM36243 (D.F.B.) and GM36238 (J.S.L.) from the National Institute of General Medical Sciences, and NSF grants CHE 9320228 (G.R.F) and CHE 9522016 (G.R.F). B.P.K. is a Department of Defense (ONR) fellow. R.J.D. acknowledges Drs. A. Shreve and R. B. Dyer for helpful discussions.

Appendix

Estimated Förster Energy-Transfer Rate. In the Förster theory (through-space) of energy transfer, the rate is given by $k_{TS} = (8.8 \times 10^{23})\kappa^2\Phi_f J n^{-4}\tau^{-1}R^{-6}$, where κ^2 is an orientation factor, Φ_f is the fluorescence quantum yield of the donor in the absence of the acceptor, J is the spectral overlap term (in $\text{cm}^6\ \text{mmol}^{-1}$), n is the solvent refractive index, τ is the donor fluorescence lifetime (in ns) in the absence of the acceptor, and R is the donor−acceptor center-to-center distance (in Å).[63] Based on known extinction coefficients, the spectral overlap term (J) for transfer in toluene from the Zn porphyrin to the Fb porphyrin is $2.94 \times 10^{-14}\ \text{cm}^6\ \text{mmol}^{-1}$ (ZnFbU, ZnFbP) and $3.53 \times 10^{-14}\ \text{cm}^6\ \text{mmol}^{-1}$ (ZnFbD, ZnFbB). These values are similar to those obtained for other Zn and Fb porphyrins.[4,11,15,17,22,64] These slight differences in J values largely reflect differences in extinction coefficients determined for the respective Fb porphyrins (FbU $\epsilon_{550} = 7800\ \text{M}^{-1}\ \text{cm}^{-1}$; FbH $\epsilon_{550} = 8900\ \text{M}^{-1}\ \text{cm}^{-1}$). In the diarylethyne-linked dimers, the Zn and Fb porphyrins have center-to-center distances (R) of ∼20 Å. The κ^2 term provides a measure of the relative orientation of the donor−acceptor transition dipoles. The Zn porphyrin is a planar oscillator and the Fb porphyrin is a linear oscillator with the transition dipole moment located along the N−N diagonal axis in the plane of the porphyrin.[65] For the case of free internal rotation about a linker that is attached to the porphyrin *meso*-carbons, the κ^2 term ranges from 1.25 (coplanar porphyrins) to 1.00 (perpendicular porphyrins) and in the dynamically averaged limit equals 1.125.[66] Using these values and the known Φ_f values of the Fb porphyrins, the calculated through-space energy-transfer efficiencies in toluene are 75% (ZnFbU, ZnFbP) and 80% (ZnFbD, ZnFbB).

There are several assumptions in this Förster energy-transfer calculation. First, we assume the conformationally averaged dynamic limit where each donor−acceptor pair samples all internal rotation angles about the cylindrically symmetric ethyne bond. Regardless, a maximum 25% variation due to porphyrin−porphyrin dihedral angle is possible in the through-space energy-transfer rate, as indicated by the 1.00 to 1.25 range in κ^2. Second, we ignore the effects of bending about the diarylethyne linkage[41] on the value of κ^2. Finally, we do not consider corrections to the point-dipole approximation (such as point-monopoles) which become important when the donor−acceptor distance is comparable to the size of the donor−acceptor π-systems, as shown for energy transfer between chlorophylls.[58] Under these assumptions, the expected k_{TS} values fall in the range of $(620\ \text{to}\ 820\ \text{ps})^{-1}$ for the four ZnFb dimers. Given the assumptions in the calculation, the average rate $(720\ \text{ps})^{-1}$ is used for all four dimers.

JA961612F

(62) Jimenez, R.; Dikshit, S. N.; Bradforth, S. E.; Fleming, G. R. *J. Phys. Chem.* **1996**, *100,* 6825−6834.

(63) Lamola, A. A. In *Energy Transfer and Organic Photochemistry*; Lamola, A. A., Turro, N. J., Eds.; Interscience: New York, 1969; p 17.

(64) Sessler, J. L. Wang, B.; Harriman, A. *J. Am. Chem. Soc.* **1995**, *117*, 704−714.

(65) Gurinovich, G. P.; Sevchenko, A. N.; Solov'ev, K. N. *Opt. Spectrosc.* **1961**, *10*, 396. Gouterman, M.; Stryer, L. *J. Chem. Phys.* **1962**, *37*, 2260.

(66) Dale, R. E.; Eisinger, J. *Biopolymers* **1974**, *13*, 1573−1605.